Trabecular Bone Microarchitecture and Characteristics in Different Regions of the Glenoid

Article *in* Orthopedics · March 2015
DOI: 10.3928/01477447-20150305-52

CITATIONS
3

READS
45

8 authors, including:


Xinning Li
Boston University
104 PUBLICATIONS **867** CITATIONS
SEE PROFILE


Emily Curry
Boston University
32 PUBLICATIONS **125** CITATIONS
SEE PROFILE


Daniel Choi
Hospital for Special Surgery
35 PUBLICATIONS **784** CITATIONS
SEE PROFILE


Edward V Craig
Hospital for Special Surgery
130 PUBLICATIONS **3,450** CITATIONS
SEE PROFILE

Trabecular Bone Microarchitecture and Characteristics in Different Regions of the Glenoid

XINNING LI, MD; PHILLIP WILLIAMS, MD; EMILY J. CURRY, BA; DANIEL CHOI, MENG; EDWARD V. CRAIG, MPH, MD; RUSSELL F. WARREN, MD; LAWRENCE V. GULOTTA, MD; TIMOTHY WRIGHT, PHD

abstract

Success of shoulder surgery depends on implant fixation to the glenoid trabecular bone. The purpose of this study was to evaluate the anatomic characteristics of the normal glenoid trabecular bone microarchitecture to help assist in implant design and provide data for finite element analyses. Eight cadavers without evidence of osteoarthritis were used. Glenoids were scanned with micro-computed tomography and then divided into lateral and medial, then superior, inferior, anterior, and posterior quadrants (8 total segments). Each segment was analyzed for total mineral density, bone volume fraction, structure model index, and trabecular thickness (Tb.Th), number (Tb.N), and separation. Bone volume fraction was significantly higher ($P<.05$) in the posterolateral (20.8%±4.5%) and posteromedial (18.6%±2.5%) regions. Both Tb.N and Tb.Th were also highest in the posterolateral (Tb.N, 1.74±0.374 mm; Tb.Th, 0.148±0.017 mm) and posteromedial (Tb.N, 1.49±0.401 mm; Tb.Th, 0.165±0.016 mm) regions. Trabecular separation was greatest in the superomedial segment (1.00±0.181 mm) and lowest in the posterolateral region (0.663±0.121 mm). For structural model index, both the posterolateral (0.314) and posteromedial (0.312) regions had lower values than the other regions. The posterior segment of the normal glenoid in both the lateral and medial regions has the highest density, which is attributed to the increased trabecular number and thickness with decreased separation. This increased density may be attributed to the posterior directed loading of the glenohumeral joint. The trabecular microarchitecture in the glenoid is plate-like, as indicated by the low structural model index.[*Orthopedics*. 2015; 38(3):e163-e168.]

The authors are from the Department of Orthopaedic Surgery (XL), Boston University School of Medicine, Boston, Massachusetts; and the Hospital for Special Surgery (PW, EJC, DC, EVC, RFW, LVG, TW), New York, New York.

Dr Williams, Ms Curry, Mr Choi, and Dr Wright have no relevant financial relationships to disclose. Dr Li is a paid consultant for DePuy-Mitek Sports Medicine and Tornier. Dr Craig is a paid consultant for and receives royalties from Biomet. Dr Warren is a paid consultant for Biomet and Ivy Sports. Dr Gulotta is a paid consultant for and is on the speaker's bureau of Biomet.

The authors thank Lyudmila Lukashova for her work in scanning the glenoid specimens on the MicroCT machine.

Correspondence should be addressed to: Xinning Li, MD, Department of Orthopaedic Surgery, Boston University School of Medicine, 720 Harrison Ave, Ste 808, Boston, MA 02118 (xinning.li@gmail.com).

Received: February 3, 2014; Accepted: May 13, 2014.

doi: 10.3928/01477447-20150305-52

Technique and implant technology in shoulder surgery has advanced significantly over the past decade.[1] Bankart[2] described the first capsulolabral repair with reattachment of the soft tissue onto the glenoid rim for shoulder instability in 1938. Since that time, various techniques and labral fixation implants have been reported in literature.[3-7] Success of anchor fixation and pullout strength rely on the quality of the bone microarchitecture.[8,9] Similarly, total shoulder arthroplasty (TSA) was first introduced by Neer[10] in the 1970s and has evolved into a well-established treatment method for shoulder arthritis and many other shoulder pathologies.[11]

Most patients achieve significant improvement in shoulder function along with decreased pain and better overall physical well-being after the procedure.[12] Complications are rare; however, glenoid loosening remains the main concern that may result in revision surgery and deterioration in quality of life.[13-16] Factors associated with glenoid loosening include the amount of bone ingrowth for cementless glenoid components, cement-to-bone interdigitation and cement technique for cemented components,[17] eccentric loading of the glenoid component,[13,14] and infection. Most of these factors are highly dependent on the quality of the glenoid bone and especially on the microarchitecture of the trabecular bone. In addition, soft tissue balancing, implant version, implant size, and quality of the rotator cuff musculature are also important factors affecting implant survival and longevity in TSA.

Several investigators reported on glenoid bone mineral density in both cortical and cancellous regions.[18-22] These studies were typically done with low-resolution micro-computed tomography (microCT) and reported higher bone mineral density in the upper and posterior regions of the glenoid.[18,23,24] Mechanical properties of different regions of the glenoid were also investigated[20,22,24-26] using techniques such as ultrasound,[27] indentation,[26] and direct compression testing.[22,23] These studies reported variation in the mechanical properties in the same glenoid regions, which may be due to the differences in cadaver ages, techniques, or measurement protocols.[22]

Whereas the mechanical properties of the cortical bone are relatively consistent, the properties of the trabecular bone are varied. To design a successful glenoid component or suture anchor, it is essential to understand the characteristics and microarchitecture of the trabecular bone. Poor bone quality is a major contributor to glenoid component loosening in TSA. Thus, the current authors evaluated the characteristics of the glenoid trabecular bone microarchitecture using high-resolution microCT images (18.5 µm) and 3-dimensional (3-D) reconstructions. The data obtained from this study can be applied to future research aimed at improving implant fixation and can also assist in finite element analysis to discover alternative designs.

Materials and Methods

Human glenoids were obtained from 8 fresh-frozen unpaired cadaver shoulders (4 men and 4 women; average age, 75±13 years; 4 right and 4 left shoulders). The specimens included the clavicle, scapula, humerus, and surrounding soft tissue. Specimens were stored in a -20°C freezer and thawed to room temperature for 24 hours before dissection. All soft tissues were removed by sharp dissection, with careful attention not to damage the glenoid. The glenoid was then exposed after disarticulation of the clavicle and the humeral head from the glenohumeral joint. None of the glenoids had visual signs of osteoarthritis or other cartilage damage. No osteophytes were detected on the glenoid or the humeral side of the shoulder joint, and no morphological abnormalities (eg, glenoid hypoplasia) were observed. Subsequently, after removing the coracoid process at the base, a sagittal saw was used to separate the glenoid at the neck and bottom of the glenoid vault. Capsulolabral tissue was dissected off the rim of the glenoid with a scalpel. Care was taken to ensure that the orientation of each specimen was recorded.

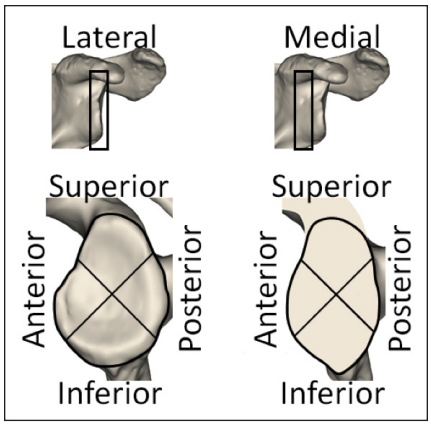

Figure 1: Division of the glenoid into the medial and lateral regions along with superior, inferior, anterior, and posterior segments. A total of 8 different segments were analyzed.

Each specimen was then scanned in 70% ethanol with microCT (Scanco µCT 35 system; Scanco Medical AG, Bassersdorf, Switzerland) at a resolution setting of 18.5 µm voxel size, 55 kVp, and 0.36° rotation step. A 180° angular range and a 400-ms exposure per view were used. The manufacturer's software was used for 3-D reconstruction of each image. Using the 3-D reconstruction, each glenoid was divided into medial and lateral regions or segments. This was accomplished by dividing the medial-to-lateral distance of the glenoid vault with the image-processing software into 2 halves of the exact same size (glenoid vault distance medial-to-lateral/2). Subsequently, superior, inferior, posterior, and anterior quadrants of the glenoid were divided into 8 total segments (**Figure 1**): superolateral, superomedial, inferolateral, inferomedial, anterolateral, anteromedial, posterolateral, and posteromedial. The trabecular bone volume was defined digitally by separating the cortical shell via manually outlining the corticocancellous boundary, and the cortical bone region was subtracted from each

Table

Glenoid Trabecular Bone Microarchitecture and Characteristics of Each Segment

Glenoid Segment (N=8)	BV/TV, %	TMD, g/cm^2	Tb.N, 1/mm^1	Tb.Th, mm	Tb.Sp, mm	SMI
Superolateral	15.6±1.8	799.7±10.7	1.47±0.227	0.141±0.011	0.750±0.109	1.06±.231
Superomedial	10.8±1.2	783.5±9.6	1.17±0.277	0.138±0.023	1.00±0.181	1.33±0.262
Inferolateral	13.3±3.6	789.6±10.7	1.35±0.313	0.129±0.008	0.821±0.146	1.13±0.291
Inferomedial	12.2±3.7	789.5±11.6	1.29±0.288	0.133±0.017	0.866±0.168	1.22±0.387
Anterolateral	14.6±4.4	796.9±12.5	1.48±0.369	0.129±0.010	0.758±0.152	1.15±0.309
Anteromedial	10.6±3.9	784.3±15.5	1.14±0.327	0.137±0.013	0.985±0.199	1.51±0.421
Posterolateral	20.8±4.5	802.0±12.8	1.74±0.374	0.148±0.017	0.663±0.121	0.314±0.415
Posteromedial	18.6±2.5	805.2±16.0	1.49±0.401	0.165±0.016	0.803±0.170	0.312±0.289
P	.002	.011	.027	.001	.002	<.001

Abbreviations: BV/TV, bone volume fraction; SMI, structural model index; Tb.N, trabecular number; Tb.Sp, trabecular separation; Tb.Th, trabecular thickness; TMD, total mineral density.

segment again using the manufacturer's software.

Subsequent detailed analysis of each segment's trabecular microarchitecture included total mineral density (TMD), bone volume fraction (BV/TV), trabecular thickness (Tb.Th), trabecular number (Tb.N), trabecular separation (Tb.Sp), and structure model index (SMI).[1] Total mineral density is the calculation of the total mineral density of each trabecular region of interest reported as g/cm^2. Bone volume fraction is the ratio of the segmented bone volume to the total volume of the region of interest reported as a percentage. Trabecular number is the measure of the average number of trabeculae per unit of length reported as 1/mm. Both trabecular thickness and separation are reported in millimeters and accessed using direct 3-D methods. Trabecular thickness is reported as the mean of the specific region, and trabecular separation is the mean distance between each trabeculae. The SMI is an indicator of the trabeculae structure, varying from 0 for parallel plates to 3 for cylindrical rods. All numbers were reported as an average (N=8) with 1 SD.

Analysis of variance was used to examine whether a difference existed among the mean values of the segments for each microCT measurement. The Bonferroni post-hoc technique was used for multiple comparisons. A *P* value of .05 or less was considered significant. SPSS version 12 statistical software (IBM, Armonk, New York) was used for all calculations.

Results

Bone volume fraction was significantly higher (*P*<.05) in the posterolateral (20.8%±4.5%) and posteromedial (18.6%±2.5%) segments compared with all other segments. In contrast, BV/TV in the superomedial area (10.8%±1.2%) was significantly lower (*P*<.05) (**Figure 1**). Total mineral density was highest in the posteromedial (805.2±16.0 g/cm^2) and posterolateral (802.0±12.8 g/cm^2) segments. Total mineral density was lowest in the superomedial (783.5±9.6 g/cm^2) and anteromedial (784.3±15.5 g/cm^2) segments.

Both Tb.N and Tb.Th were highest in the posterolateral (Tb.N, 1.74±0.374 mm; Tb.Th, 0.148±0.017 mm) and posteromedial (Tb.N, 1.49±0.401 mm; Tb.Th, 0.165±0.016 mm) segments. In contrast, the inferolateral (0.129±0.008 mm) and anterolateral (0.129±0.010 mm) segments had the lowest trabecular thickness. Trabecular separation was highest in the superomedial segment (1.00±0.181 mm) and lowest in the posterolateral segment (0.663±0.121 mm). Structure model index was highest in the anteromedial segment (1.51±0.42), whereas both the posterolateral (0.314±0.415) and posteromedial (0.312±0.289) segments had lower values than the other segments. The **Table** and **Figure 2** provide complete study results.

Discussion

In this study, the posterior segment of the glenoid in both the lateral and medial regions had the highest BV/TV and TMD, as well as an increased Tb.N and Tb.Th and decreased Tb.Sp. The BV/TV was also significantly higher in the posterolateral and posteromedial segments. In contrast, the lowest TMD and BV/TV were seen in the superomedial segment (**Table**; **Figure 2**). Similar to these results, a previous study found glenoid total bone mineral density and trabecular bone mineral density to be greater posteriorly than anteriorly.[18] Frich et al[25] also reported that the greatest glenoid density was in the posterior region vs the anterior region, with a ratio of 2:1.

As in the other joints in the body, the architecture of the subchondral plate and the cancellous bone adapts to mechani-

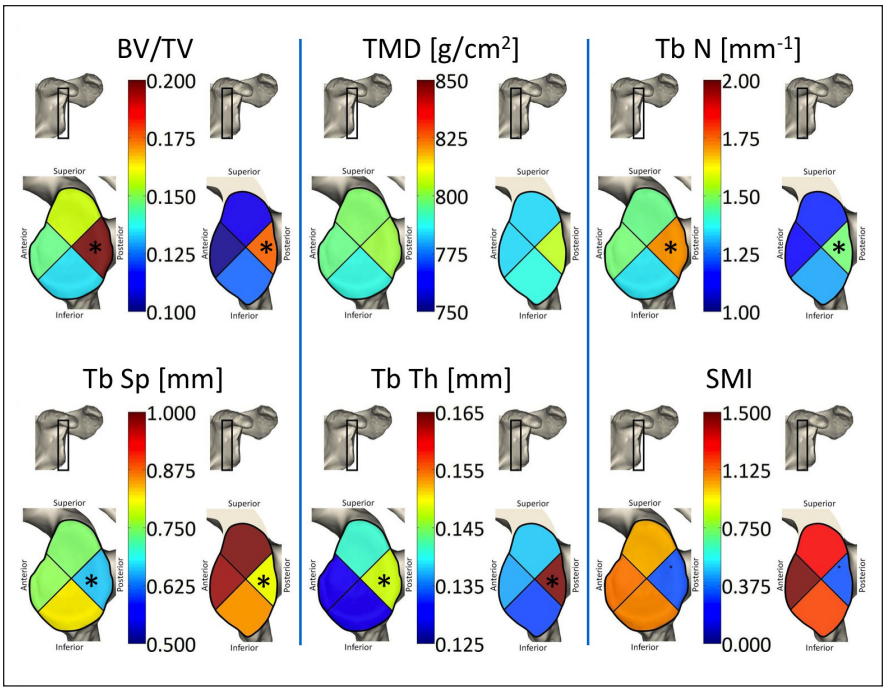

Figure 2: Detailed analysis of each segment of the glenoid as represented by color mapping. Asterisks indicate regions that are significantly different from others. Abbreviations: BV/TV, bone volume fraction; SMI, structural model index; Tb N, trabecular number; Tb Sp trabecular separation; Tb Th, trabecular thickness; TMD, total mineral density.

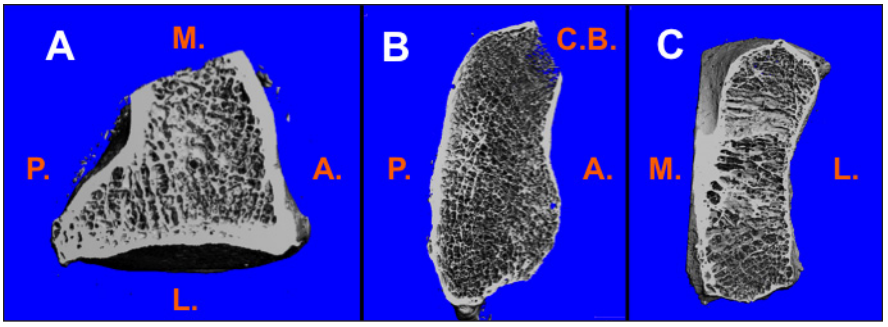

Figure 3: Micro-computed tomography image of a 56-year-old male glenoid demonstrating the thicker trabecular density (A and B), decreased separation (A and B), and plate-like structure (C) in the posterior region. Abbreviations: A, anterior; C.B., coracoid base; L, lateral; M, medial; P, posterior.

cal load.[28-30] Higher loads are exhibited in the posterior glenoid vault,[23] consistent with biomechanical studies that showed that trabecular bone is denser in regions of high shear stress.[27,31] Using a stereophotogrammetric technique to quantify contact patterns in the glenoid, Soslowsky et al[32] illustrated a posterior shift in the glenoid contact area as the humeral head was elevated and abducted. In a glenohumeral biomechanical model, Gupta and Lee[33] also found that posteriorly directed forces and contact pressures were significantly increased in overhead activities. In contrast to these studies, Bey et al[34] evaluated in vivo glenohumeral joint contact patterns in patients with a combined 3-D bone model and joint motion data. They reported that at baseline, the glenoid contact center is always located in the posterior region of the glenoid. With arm abduction, significant changes to the contact center occur in a superior-to-inferior direction, not an anterior-to-posterior direction as reported by Soslowsky et al.[32] Boyer et al[35] also supported the findings of Bey et al[34] with in vivo orthogonal fluoroscopic images and magnetic resonance imaging computer models that showed that the centroid of contact on the glenoid is always more than 5 mm posterior from the geometric center of the glenoid. These in vivo contact patterns help explain the finding that the posterolateral and posteromedial segments had the highest BMD and BV/TV, whereas the superomedial segment had the lowest values. It appears that even in the normal shoulder without evidence of osteoarthritis, the normal force and loading pattern is directed posterior on the glenoid, resulting in the higher density in the posterior (medial and lateral) segments.

Cancellous bone strength reflects a combination of density and microarchitecture.[33,36-38] Bone volume fraction is correlated with other structural properties such as Tb.Sp, Tb.Th, and Tb.N.[38,39] In a microCT analysis of cadaver calcanei, Mittra et al[20] showed that Tb.N and Tb.Sp and connectivity density had the strongest correlations. More importantly, these 3 indices were also significantly correlated to ultimate strength and outperformed bone mineral density as a predictor. As trabeculae are lost, connectivity decreases and trabecular separation increases. However, Tb.Th was not significantly correlated to any of the other trabecular indices. There is evidence that mechanical augmentation of bone results in a thickening of existing trabeculae without increasing the number of trabeculae.[20,21,40] However, bone loss reduces the number of trabeculae without decreasing the thickness of trabeculae. Despite this finding, ultimate bone strength is still better correlated with Tb.N than with Tb.Th. Several studies reported the ultimate strength of bone in the glenoid as ranging from 10.3 to 110 MPa, with the strongest bone in the posterosuperior[19,25,26] or posterocentral regions.[27]

The lowest strength was typically found in the anteroinferior region,[22,25,26] which is consistent with the current authors' microarchitecture results (anteromedial and anterolateral segments). The large variation in the reported ultimate strength is likely due to the differences in cadaver age and mechanical testing techniques. Bone elastic modulus was shown to decrease in up to 80% of specimens from the age of 20 to 80 years.[41-44]

Looking at trabeculae microarchitecture, both the posterolateral and posteromedial segments had the highest Tb.N and Tb.Th. However, the Tb.Sp was significantly lower in the posterolateral segment (0.66±0.12) compared with all other segments. The posterolateral region is located directly under the subchondral surface and experiences the most load from the humeral head. This explains the significantly increased Tb.N (1.7±0.37) with decreased Tb.Th (0.15±0.02) and Tb.Sp. The increased number of trabeculae in this segment is likely in direct adaptive response to the increased load transferred through this region of the glenoid. The fact that Tb.N and Tb.Th were increased posteriorly in both the lateral and medial regions is also consistent with the known loading patterns of the glenohumeral joint. Furthermore, patients with capsulorrhaphy arthropathy secondary to overtightening of the anterior capsule or primary osteoarthritis will further move the center of rotation posteriorly, which is responsible for the posteriorly directed wear patterns and trabecular microarchitecture.[1] The higher Tb.Th represents mechanical adaptation of the posterior glenoid bone in response to higher loads. The posterior glenoid also has a higher Tb.N and therefore would be expected to possess the highest ultimate strength. The decreased Tb.Sp posteriorly is a natural consequence of the increased number of trabeculae in the same space, thus resulting in increased TMD and BV/TV.

The overall SMI[1] of the glenoids was between 0.3 and 1.5 and was significantly lower in the posterolateral (0.3) and posteromedial (0.3) segments compared with the other segments. Thus, the morphology of the glenoid trabecular bone is more plate-like than cylindrical rods and oriented perpendicular to the subchondral bone with thin rods interconnecting the plates. However, progressing from the posterolateral/posteromedial region to the anteromedial/anterolateral region, the morphology becomes less plate-like as more rods are seen on the 3-D images, consistent with the increasing SMI (**Figure 3**; **Table**). This plate-like morphology has also been described by Frich et al.[23]

A limitation of the current study is the ages of the cadavers from which the authors extracted the glenoids. Although none of the cadavers had visual evidence of osteoarthritis, due to their advanced age, the donors may have had early-onset osteoarthritis and posterior humeral head subluxation that would have altered the contact pattern to shift posteriorly, thus resulting in the higher density seen in the posteromedial and posterolateral regions. However, no posterior cartilage wear was evident on visual inspection, and several studies support the finding that the native glenohumeral contract region is located primarily in the posterior aspects of the glenoid.[32-35] Future studies will focus on trabecular bone analysis in the arthritic glenoid and will be evaluated based on the amount of retroversion and glenoid morphology.

Conclusion

The posteromedial and posterolateral segments of a normal nonarthritic glenoid exhibited the highest TMD, Tb.N, and Tb.Th and a decreased Tb.Sp. This finding supports the theory that the normal shoulder kinematics and glenohumeral joint loading are predominantly in the posterior aspect of the glenoid. Furthermore, the posterior region is also more plate-like than the anterior region. Future designs of glenoid implants or suture anchors should account for the distinct differences in the trabecular microarchitecture between different regions of the glenoid.

References

1. Parsons IM, Buoncristiani AM, Donion S, Campbell B, Smith KL, Matsen FA III. The effect of total shoulder arthroplasty on self-assessed deficits in shoulder function in patients with capsulorrhaphy arthropathy. *J Shoulder Elbow Surg*. 2007; 16(3 suppl):S19-S26.
2. Bankart ASB. The pathology and treatment of recurrent dislocation of the shoulder joint. *Br J Surg*. 1938; 26:23-29.
3. Kokubu T, Nagura I, Mifune Y, Kurosaka M. Arthroscopic bony Bankart repair using double-threaded headless screw: a case report. *Case Rep Orthop*. 2012;2012:789418.
4. Ahmed I, Ashton F, Robinson CM. Arthroscopic Bankart repair and capsular shift for recurrent anterior shoulder instability: functional outcomes and identification of risk factors for recurrence. *J Bone Joint Surg Am*. 2012; 94(14):1308-1315.
5. Zaffagnini S, Marcheggiani Muccioli GM, Giordano G, et al. Long-term outcomes after repair of recurrent post-traumatic anterior shoulder instability: comparison of arthroscopic transglenoid suture and open Bankart reconstruction. *Knee Surg Sports Traumatol Arthrosc*. 2012; 20(5):816-821.
6. Iwaso H, Uchiyama E, Sakakibara S, Fukui N. Modified double-row technique for arthroscopic Bankart repair: surgical technique and preliminary results. *Acta Orthop Belg*. 2011; 77(2):252-257.
7. Zhu YM, Lu Y, Zhang J, Shen JW, Jiang CY. Arthroscopic Bankart repair combined with remplissage technique for the treatment of anterior shoulder instability with engaging Hill-Sachs lesion: a report of 49 cases with a minimum 2-year follow-up. *Am J Sports Med*. 2011; 39(8):1640-1647.
8. Roth CA, Bartolozzi AR, Ciccotti MG, et al. Failure properties of suture anchors in the glenoid and the effects of cortical thickness. *Arthroscopy*. 1998; 14(2):186-191.
9. Tingart MJ, Apreleva M, Lehtinen J, Zurakowski D, Warner JJ. Anchor design and bone mineral density affect the pull-out strength of suture anchors in rotator cuff repair: which anchors are best to use in patients with low bone quality? *Am J Sports Med*. 2004; 32(6):1466-1473.
10. Neer CS II. Replacement arthroplasty for glenohumeral osteoarthritis. *J Bone Joint Surg Am*. 1974; 56(1):1-13.
11. Neer CS II, Watson KC, Stanton FJ. Recent experience in total shoulder replacement. *J Bone Joint Surg Am*. 1982; 64(3):319-337.
12. Carter MJ, Mikuls TR, Nayak S, Fehringer

EV, Michaud K. Impact of total shoulder arthroplasty on generic and shoulder-specific health-related quality-of-life measures: a systematic literature review and meta-analysis. *J Bone Joint Surg Am*. 2012; 94(17):e127.

13. Bohsali KI, Wirth MA, Rockwood CA Jr. Complications of total shoulder arthroplasty. *J Bone Joint Surg Am*. 2006; 88(10):2279-2292.
14. Chin PY, Sperling JW, Cofield RH, Schleck C. Complications of total shoulder arthroplasty: are they fewer or different? *J Shoulder Elbow Surg*. 2006; 15(1):19-22.
15. Wirth MA, Rockwood CA Jr. Complications of total shoulder-replacement arthroplasty. *J Bone Joint Surg Am*. 1996; 78(4):603-616.
16. Cofield RH, Edgerton BC. Total shoulder arthroplasty: complications and revision surgery. *Instr Course Lect*. 1990; 39449-39462.
17. Nyffeler RW, Meyer D, Sheikh R, Koller BJ, Gerber C. The effect of cementing technique on structural fixation of pegged glenoid components in total shoulder arthroplasty. *J Shoulder Elbow Surg*. 2006; 15(1):106-111.
18. Lehtinen JT, Tingart MJ, Apreleva M, Warner JJ. Total, trabecular, and cortical bone mineral density in different regions of the glenoid. *J Shoulder Elbow Surg*. 2004; 13(3):344-348.
19. Mimar R, Limb D, Hall RM. Evaluation of the mechanical and architectural properties of glenoid bone. *J Shoulder Elbow Surg*. 2008; 17(2):336-341.
20. Mittra E, Rubin C, Gruber B, Qin YX. Evaluation of trabecular mechanical and microstructural properties in human calcaneal bone of advanced age using mechanical testing, microCT, and DXA. *J Biomech*. 2008; 41(2):368-375.
21. Mittra E, Rubin C, Qin YX. Interrelationship of trabecular mechanical and microstructural properties in sheep trabecular bone. *J Biomech*. 2005; 38(6):1229-1237.
22. Kalouche I, Crepin J, Abdelmoumen S, Mitton D, Guillot G, Gagey O. Mechanical properties of glenoid cancellous bone. *Clin Biomech (Bristol, Avon)*. 2010; 25(4):292-298.
23. Frich LH, Odgaard A, Dalstra M. Glenoid bone architecture. *J Shoulder Elbow Surg*. 1998; 7(4):356-361.
24. Couteau B, Mansat P, Darmana R, Mansat M, Egan J. Morphological and mechanical analysis of the glenoid by 3D geometric reconstruction using computed tomography. *Clin Biomech (Bristol, Avon)*. 2000; 15(suppl):S8-S12.
25. Frich LH, Jensen NC, Odgaard A, Pedersen CM, Sojbjerg JO, Dalstra M. Bone strength and material properties of the glenoid. *J Shoulder Elbow Surg*. 1997; 6(2):97-104.
26. Anglin C, Tolhurst P, Wyss UP, Pichora DR. Glenoid cancellous bone strength and modulus. *J Biomech*. 1999; 32(10):1091-1097.
27. Mansat P, Barea C, Hobatho MC, Darmana R, Mansat M. Anatomic variation of the mechanical properties of the glenoid. *J Shoulder Elbow Surg*. 1998; 7(2):109-115.
28. Eckstein F, Muller-Gerbl M, Steinlechner M, Kierse R, Putz R. Subchondral bone density in the human elbow assessed by computed tomography osteoabsorptiometry: a reflection of the loading history of the joint surfaces. *J Orthop Res*. 1995; 13(2):268-278.
29. Muller-Gerbl M, Putz R, Kenn R. Demonstration of subchondral bone density patterns by three-dimensional CT osteoabsorptiometry as a noninvasive method for in vivo assessment of individual long-term stresses in joints. *J Bone Miner Res*. 1992; 7(suppl 2):S411-S418.
30. Simkin PA, Heston TF, Downey DJ, Benedict RS, Choi HS. Subchondral architecture in bones of the canine shoulder. *J Anat*. 1991; 175:213-227.
31. Diduch DR, Tadje JP, Ferguson RE Jr, Edlich RF. Modern concepts in arthroscopic Bankart repair. *J Long Term Eff Med Implants*. 1999; 9(4):377-393.
32. Soslowsky LJ, Flatow EL, Bigliani LU, Pawluk RJ, Ateshian GA, Mow VC. Quantitation of in situ contact areas at the glenohumeral joint: a biomechanical study. *J Orthop Res*. 1992; 10(4):524-534.
33. Gupta R, Lee TQ. Positional-dependent changes in glenohumeral joint contact pressure and force: possible biomechanical etiology of posterior glenoid wear. *J Shoulder Elbow Surg*. 2005; 14(1 suppl):105S-110S.
34. Bey MJ, Kline SK, Zauel R, Kolowich PA, Lock TR. In vivo measurement of glenohumeral joint contact patterns. *EURASIP J Adv Signal Process*. 2010 Jan 1;2010.
35. Boyer PJ, Gill TJ, Papannagari R, Stewart SL, Warner JJ, Li G. In vivo articular cartilage contact at the glenohumeral joint: preliminary report. *J Orthop Sci*. 2008; 13(4):359-365.
36. Mosekilde L. Age-related changes in vertebral trabecular bone architecture: assessed by a new method. *Bone*. 1988; 9(4):247-250.
37. Mosekilde L, Vildik A, Mosekilde L. Correlation between the compressive strength of iliac and vertebral trabecular bone in normal individuals. *Bone*. 1985; 6(5):291-295.
38. Thomsen JS, Ebbesen EN, Mosekilde L. Relationships between static histomorphometry and bone strength measurements in human iliac crest bone biopsies. *Bone*. 1998; 22(2):153-163.
39. Goulet RW, Goldstein SA, Ciarelli MJ, Kuhn JL, Brown MB, Feldkamp LA. The relationship between the structural and orthogonal compressive properties of trabecular bone. *J Biomech*. 1994; 27(4):375-389.
40. Rubin C, Turner AS, Muller R, et al. Quantity and quality of trabecular bone in the femur are enhanced by a strongly anabolic, noninvasive mechanical intervention. *J Bone Miner Res*. 2002; 17(2):349-357.
41. Ding M. Age variations in the properties of human tibial trabecular bone and cartilage. *Acta Orthop Scand Suppl*. 2000; 292:1-45.
42. Ding M, Dalstra M, Danielsen CC, Kabel J, Hvid I, Linde F. Age variations in the properties of human tibial trabecular bone. *J Bone Joint Surg Br*. 1997; 79(6):995-1002.
43. Chalmers J, Weaver JK. Cancellous bone: its strength and changes with aging and an evaluation of some methods for measuring its mineral content: II. An evaluation of some methods for measuring osteoporosis. *J Bone Joint Surg Am*. 1966; 48(2):299-308.
44. Weaver JK, Chalmers J. Cancellous bone: its strength and changes with aging and an evaluation of some methods for measuring its mineral content. *J Bone Joint Surg Am*. 1966; 48(2):289-298.